Molecular Vision 2020; 26:517-529 <http://www.molvis.org/molvis/v26/517>
Received 21 October 2019 | Accepted 27 July 2020 | Published 29 July 2020

Interleukin-6 promotes proliferative vitreoretinopathy by inducing epithelial-mesenchymal transition via the JAK1/STAT3 signaling pathway

Xiaoyun Chen, Weimin Yang, Xiaoqian Deng, Shaobi Ye, Wei Xiao

State Key Laboratory of Ophthalmology, Zhongshan Ophthalmic Center, Sun Yat-sen University, Guangzhou, China

Purpose: Interleukin-6 (IL-6) is elevated in intraocular fluid from eyes with proliferative vitreoretinopathy (PVR), but the exact role of the cytokine is still unclear. We investigated the function and mechanism of IL-6 in retinal pigment epithelium (RPE) cell biology in vitro and in a mouse model in vivo.

Methods: After treatment with various concentrations of IL-6, RPE cell proliferation was assessed with cell counting kit-8 (CCK-8) assay, and epithelial-mesenchymal transition (EMT) markers were evaluated using western blotting and immunofluorescent staining. The activation of JAK1/STAT3 signaling was determined with western blotting. Moreover, the effects of blockade of IL-6/JAK1/STAT3 signaling were investigated using pharmacological inhibitor S3I-201. For in vivo studies, the PVR model was induced with intravitreal injection of dispase/collagenase in wild-type and IL-6 knockout mice. The severity of PVR was evaluated with histological analysis. The expression of IL-6, gp130, and EMT markers was assessed with quantitative real-time PCR and western blotting.

Results: IL-6 statistically significantly induced RPE cell proliferation and EMT in a dose-dependent manner in vitro, which was accompanied by rapid phosphorylation of JAK1 and STAT3. Blockade of the IL-6/JAK1/STAT3 pathway with S3I-201 apparently inhibited RPE proliferation and EMT. Furthermore, IL-6 and gp130 overexpression, and JAK1/STAT3 signaling hyperactivation were detected in the retinas of the wild-type mice at 1, 3, and 7 days after dispase/collagenase injection. Finally, we confirmed that IL-6 deficiency markedly alleviated mouse PVR development via inhibiting EMT.

Conclusions: These findings indicate that IL-6 promotes PVR by inducing RPE proliferation and EMT via the JAK1/STAT3 signaling pathway. We provided new evidence that therapeutic strategies to block IL-6 may be beneficial for PVR.

Proliferative vitreoretinopathy (PVR) is a vision-threatening complication of retinal detachment (RD), ocular trauma, and inflammatory vitreoretinopathies [1]. Despite remarkable advances in surgical technique, PVR is still a major cause of failure after RD surgery with an incidence rate of 5–10% [2]. Histologically, PVR is characterized by formation of fibrotic preretinal or subretinal membranes, or both, which mechanically drag the retina, and cause retinal redetachment [3]. Moreover, surgery for eyes with severe PVR is a huge challenge for surgeons, while the post-operative visual outcome is often unsatisfactory [4]. Several adjunctive therapeutics alleviating PVR have been developed, such as molecules targeting inflammation or cell proliferation, but clinical success is rare [4]. This could be in part due to the incomplete elucidation of PVR pathogenesis. Therefore, it is necessary to better understand the cellular and molecular mechanisms of this fibrotic event.

Correspondence to: Wei Xiao, State Key Laboratory of Ophthalmology, Zhongshan Ophthalmic Center, Sun Yat-Sen University, 54S Xianlie Road, Guangzhou 510060, China; Phone: (86) 20 87331539; FAX: (86) 20 87330341; email: xiaow27@mail.sysu.edu.cn

Several cell types, including retinal pigment epithelium (RPE) cells, retinal Müller cells, fibroblasts, macrophages, and bone marrow–derived cells, are involved in PVR pathogenesis [5]. Among them, RPE cells are considered to play the foremost role in PVR development because these cells represent the largest proportion of the cellular component of human PVR specimens [6]. Mature RPE cells are mitotically quiescent in physiologic conditions. When the neuroretina is detached, RPE cells may be exposed to the vitreous, which contains abundant cytokines and growth factors [7]. Thus, RPE cells are stimulated to detach from Bruch's membrane, to migrate into the vitreous through the retinal breaks, and to form fibrotic membranes eventually [8]. From the aspect of cell biology, activated RPE cells shift from epithelial to fibroblast-like cells, namely, epithelial-mesenchymal transition (EMT) [8]. Several previous studies have suggested that EMT of RPE cells is the main contributor of the pathogenesis of PVR [8,9]. In this regard, investigating the molecular mechanisms underlying EMT of RPE cells may be of great value in the development of agents preventing PVR.

Interleukin (IL)-6 is a pleiotropic inflammatory cytokine that has a central role in inflammatory response and malignancy [10]. On target cells, IL-6 binds to the membrane-bound

receptor (IL-6R) and subsequently, recruits the signal transducing gp130 receptor. This is known as IL-6 classic signaling, and it is restricted to cells expressing membrane-bound IL-6R, such as hepatocytes, macrophages, neutrophils, and some T-cell subsets [11]. In addition, IL-6 can alternatively bind to soluble receptor (sIL-6R) and induce intracellular signaling via gp130, which is termed trans-signaling [12]. Classic signaling is needed for regenerative and anti-inflammatory functions, whereas trans-signaling is considered to be proinflammatory in numerous chronic diseases and cancers [13-15]. Elevated concentration of IL-6 has been reported in the intraocular fluid of patients with various chorioretinal diseases, including central retinal vein occlusion [16], exudative age-related macular degeneration [17], and proliferative diabetic retinopathy [18]. Through analyzing the intraoperatively obtained subretinal fluid and vitreous, it was reported that the level of IL-6 was significantly higher in patients who developed postoperative PVR than in those with uncomplicated RD [19,20]. These findings suggest that IL-6 might be an important growth factor promoting PVR. However, the mechanism under IL-6 contributing to the pathogenesis of PVR is still poorly understood.

In the present study, we examined the functions and cellular mechanisms of IL-6 in PVR pathogenesis using the cultured RPE cell model and the PVR mouse model. We then explored whether blockade of IL-6/JAK1/STAT3 signaling and knockout of IL-6 could inhibit RPE proliferation and EMT in vitro, and alleviate PVR severity in vivo.

METHODS

Cell culture, STR analysis, and treatment: The human RPE cell line ARPE-19 was purchased from American Type Culture Collection (ATCC, Manassas, VA). The cells were maintained in Dulbecco's modified Eagle's medium (DMEM; Gibco, Life Technologies, Grand Island, NY) containing 10% fetal bovine serum (FBS; Gibco) at 37 °C in a humidified atmosphere containing 5% CO_2. The cell line was authenticated with short tandem repeat (STR) analysis. The STR results showed that the DNA of the cell line perfectly matched ARPE-19, and no cross contamination of human cells was detected (Appendix 1).

For IL-6 treatment, the cells were seeded in six- or 96-well plates and incubated with different concentrations of IL-6 (Cell Signaling, Danvers, MA). The pharmacological inhibitor of STAT3 signaling S3I-201 was purchased from Selleck Chemicals (Houston, TX), prepared in dimethyl sulfoxide (DMSO) as 10 mM stock solution, and added 60 min before treatment with IL-6.

Cell proliferation assay: To determine the effect of IL-6 on the proliferation of RPE cells, the cells were seeded into 96-well plates and treated with increasing concentrations of IL-6 (5, 10, 25, and 50 ng/ml) for 24, 48, and 72 h, respectively. At the end of the treatment period, 10 µl of cell counting kit-8 (CCK-8) mixed with 90 µl of serum-free medium was added to each well and incubated for 3 h. The absorbance (A) at 450 nm was measured using a microplate reader.

EdU staining assay: To verify the effect of S3I-201 on RPE growth, cell proliferation was determined using the Cell-Light™ EdU Apollo 488 In Vitro Kit (RiboBio, Guangzhou, China) according to the manufacturer's protocols. Briefly, RPE cells were seeded in six-well plates and exposed to IL-6 with or without S3I-201 for 48 h. The culture medium was replaced with fresh medium containing 50 µM EdU for 2 h. Then, the cells were fixed with acetone for 10 min, washed with PBS (1X; 135 mM NaCl, 4.7 mM KCl, 10 mM Na_2HPO_4, 2 mM NaH_2PO_4, pH 7.4), and sequentially incubated with Apollo reaction buffer containing FITC-fluorescein for 30 min. Finally, the cells were incubated with DAPI, mounted, and examined with a confocal microscope (LSM510; Carl Zeiss, Overkochen, Germany).

Immunofluorescence staining of cultured cells: Immunofluorescent staining of the cultured cells was performed according to previously described protocols [21]. Primary antibodies collagen type I (Abcam, Cambridge, UK), fibronectin (Abcam), N-cadherin (Abcam), and vimentin (Abcam) were used. Images were obtained with a confocal microscope (LSM510; Carl Zeiss).

Mouse model of PVR induced with dispase/collagenase intravitreal injection: All animal experiments conformed to the ARVO Statement for the Use of Animals in Ophthalmic and Vision Research, and were approved by the Animal Use and Care Committee of Zhongshan Ophthalmic Center at the Sun Yat-Sen University (Guangzhou, China). Six- to eight-week-old wild-type (WT; C57BL/6J) and IL-6 knockout (IL-$6^{-/-}$; C57BL/6J-IL-$6^{em1(Luc\text{-}eGFP)Smoc}$, Shanghai Model Organisms Center, Shanghai, China) mice were used. The mouse model of PVR was induced with intravitreal injection of dispase/collagenase (Roche, Mannheim, Germany), as previously reported with minor modifications [22]. Briefly, the WT and IL-$6^{-/-}$ mice were anesthetized with 1.5% isoflurane balanced with O_2 at a flow rate of 2 l/min, and their pupils were pharmacologically dilated. Intravitreal injection with 1 µl of dispase/collagenase at the concentration of 0.02 U/µl was made in the dorsonasal quadrant (1 o'clock) of the right eye with a Hamilton syringe, fitted with a 30 G needle. Control animals were injected with an equal volume of PBS.

Quantitative real-time PCR: Total RNA from the cultured cells and retinas was extracted using TRIzol reagent (Invitrogen, Carlsbad, CA). The quality and concentration of RNA were measured using spectrophotometry at wavelengths of 260 nm and 280 nm. cDNA was synthesized using a Prime-script™ RT Master Mix (Takara, Dalian, China) according to the manufacturer's instruction. Quantitative real-time PCR was performed using the TB Green™ Premix Ex Taq™ kit (Takara, Dalian, China). The PCR conditions were set as 30 s at 95 °C, followed by 5 s at 95 °C, 34 s at 60 °C. All PCR reactions were run on an ABI Prism 7000 sequence detection system (Applied Biosystems, Foster City, CA). Glyceraldehyde 3-phosphate dehydrogenase (GAPDH) was used as the internal control, and the $2^{-\Delta\Delta Ct}$ algorithm was introduced to compare the expression of each gene across groups.

Western blotting: Total protein from the cultured cells and retinas was extracted using RIPA reagent (Biocolor Bioscience & Technology, Shanghai, China). The protein samples were electrophoresed in sodium dodecyl sulfate-polyacrylamide gel electrophoresis (SDS–PAGE) gel and then were transferred to a polyvinylidene fluoride (PVDF) membrane. After blocking with 5% skim milk for 1 h at room temperature, the primary antibodies were incubated at 4 °C overnight. The primary antibodies included α-SMA, collagen type I, collagen type IV, fibronectin, and β-actin purchased from Abcam, and Snail, JAK1, phosphor-JAK1, JAK2, phosphor-JAK2, STAT3, and phosphor-STAT3 (Tyr705) purchased from Cell Signaling Technology (Danvers, MA). After washing with PBS containing 0.1% Tween-20 (PBST) three times, the secondary antibodies conjugated with horseradish peroxidase (HRP) were incubated at room temperature for 1 h. Protein expression was revealed using the Immobilon Western Chemiluminescent HRP Substrate kit (Millipore, Billerica, MA). Densitometric analysis was conducted with Image J software 1.51 (National Institutes of Health, Bethesda, MD). β-actin was used as loading control.

Histological analysis: Animals for histological analysis were submitted to ophthalmoscopic examination and euthanized (intraperitoneal pentobarbital injection, 100 mg/kg) at 7 days after injection. Eyes were collected and fixed in 4% paraformaldehyde (PFA) overnight. After dehydration and clarification, they were embedded in paraffin and sectioned serially at 4 μm thickness via the pupil-optic nerve plane, and then were stained with hematoxylin and eosin. The sections were evaluated with a light microscope (Carl Zeiss).

Statistical analysis: All statistical analyses were performed using SPSS 22.0 (SPSS, Chicago, IL). Data were presented as mean ± standard deviation (SD). Comparisons between two groups were performed using the Student *t* test, and comparisons between three or more groups were performed using one-way analysis of variance (ANOVA) with the Tukey-Kramer multiple comparison test. A p value of less than 0.05 was considered statistically significant.

RESULTS

IL-6 promotes RPE cell proliferation and EMT in vitro: To explore how IL-6 influences the behavior of RPE cells, we treated them with IL-6 at various concentrations (5, 10, 25, and 50 ng/ml). The effect of IL-6 on cell proliferation was determined with the CCK-8 assay at 24, 48, and 72 h after treatment. As shown in Figure 1, IL-6 did not affect RPE cell proliferation at 24 h, whereas the cytokine promoted cell proliferation in a dose-dependent manner after 48 h. Twenty-five nanograms per milliliter of IL-6 could statistically significantly increase cell viability after 48 h, and this effect was maintained until 72 h (Figure 1A). Additionally, we noted that IL-6 could stimulate morphological changes in RPE cells, transforming from an epithelial to a more mesenchymal phenotype (Figure 1B). To confirm the effect on EMT in RPE cells, we examined the expression levels of EMT markers with western blotting and immunofluorescence. As shown in Figure 1C,D and Figure 2, the results of western blotting and immunofluorescence staining concordantly showed that IL-6 treatment dramatically induced the expression of the EMT markers (α-SMA, collagen type I, collagen type IV, fibronectin, and N-cadherin) and the EMT-associated transcription factor Snail. Meanwhile, vimentin staining also revealed cytoskeletal reorganization when treated with IL-6 (Figure 2). Collectively, these data indicated that IL-6 contributes to promote RPE cell proliferation and EMT.

JAK1/STAT3 signaling is activated by IL-6 in RPE cells: A principal target of IL-6 signaling is the STAT3 transcription factor, which is activated by JAKs. A previous study demonstrated that IL-6 induces the activation of JAK/STAT3 transcription factors that regulate the proliferation of multiple tumor cells, invasiveness, and EMT [23]. Therefore, we then investigated whether the JAKs/STAT3 pathway is involved in IL-6-stimulated proliferation and EMT in RPE cells. We examined the expression of JAK1, JAK2, and STAT3 and phosphorylated JAK1, JAK2, and STAT3 in RPE cells cocultured with different concentrations of IL-6 for increasing durations with western blotting. We found that a low dose of IL-6 (5 ng/ml) could activate JAK1 and STAT3 dramatically with phosphorylation. JAK1 and STAT3 were hyperactivated by IL-6 at 15 min after stimulation and maintained after 6 h (Figure 3), whereas IL-6 had no effects on phosphorylated JAK2 (data not shown). These results revealed that activation

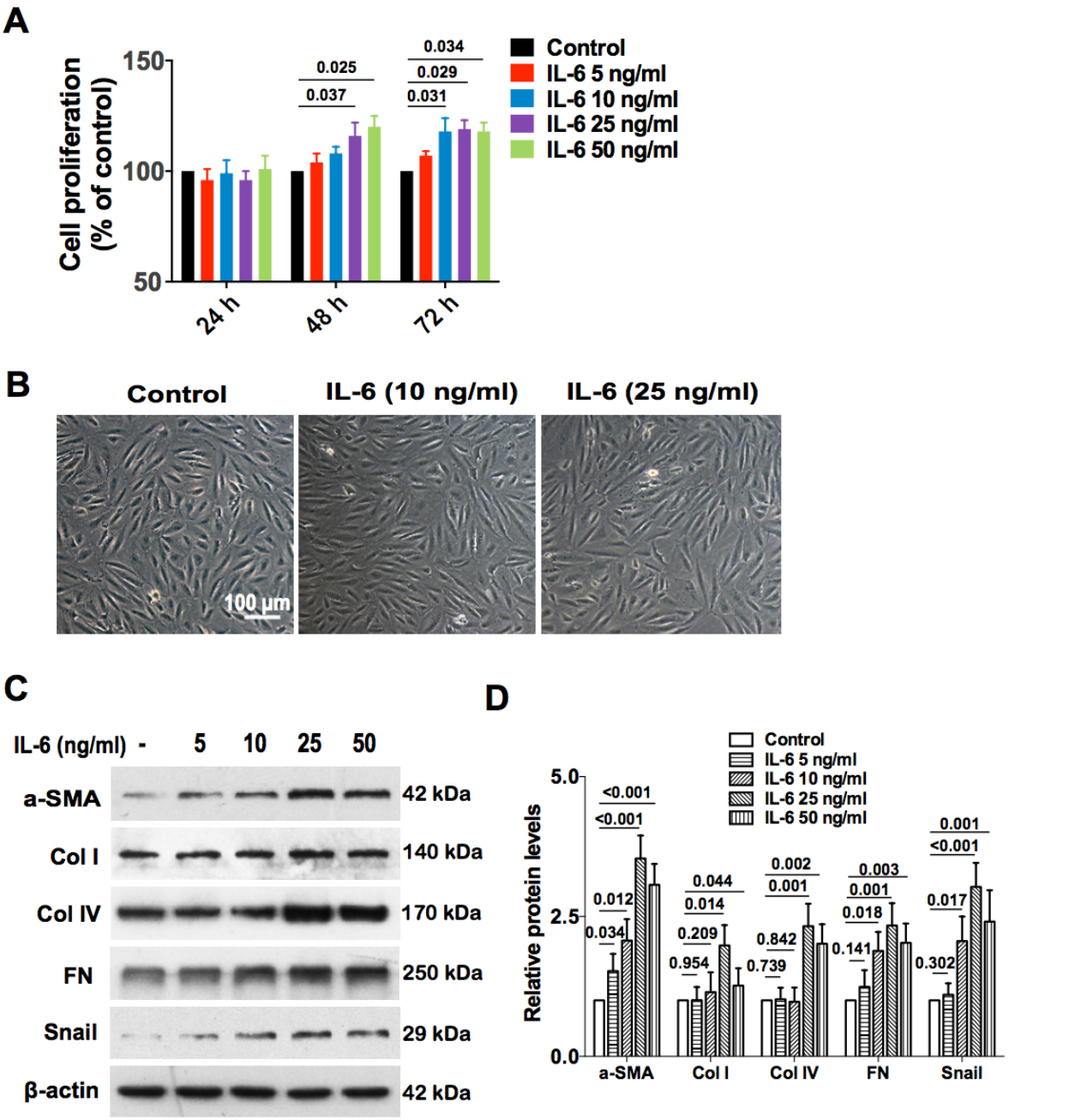

Figure 1. IL-6 promotes proliferation of RPE cells and EMT. **A**: Cell counting kit 8 (CCK-8) assay of proliferation of RPE cells after exposure to increasing concentrations of interleukin-6 (IL-6; 5, 10, 25, and 50 ng/ml) for 24, 48, and 72 h. P values versus the control group are shown (one-way analysis of variance [ANOVA] with the Tukey-Kramer multiple comparison test). **B**: Microscopic observations of RPE cells in the presence or absence of 10 and 25 ng/ml of IL-6 for 48 h. Scale bar: 100 µm. **C**: Western blotting of the expression of epithelial-mesenchymal transition (EMT) markers α-SMA, collagen type I, collagen type IV, fibronectin, and Snail after treatment with various concentrations of IL-6 (5, 10, 25, and 50 ng/ml) for 48 h. **D**: Quantification of EMT marker protein levels from three independent experiments. P values versus the control group are shown (one-way ANOVA with the Tukey-Kramer multiple comparison test).

of the JAK1/STAT3 signaling pathway is likely to be involved in IL-6-induced RPE proliferation and EMT.

EMT phenotype and proliferation are reversed by blocking IL-6/JAK1/STAT3 signaling in RPE cells: To further determine whether IL-6/JAK1/STAT3 signaling is responsible for the observed proliferation and EMT phenotype in RPE cells, we examined cell proliferation and the expression of EMT-associated proteins after IL-6/JAK1/STAT3 signaling was blocked with the pharmacological inhibitor S3I-201. EdU staining assay demonstrated that blocking of JAK1/STAT3 signaling reversed the initial increase in proliferation induced by IL-6 stimulation (Figure 4). In addition, blockade of IL-6/JAK1/STAT3 reversed IL-6 induced EMT-phenotype change, and the RPE cells retained their epithelial morphology (Figure 5A). Furthermore, the immunofluorescence and western blotting results revealed that the upregulation of EMT markers α-SMA, collagen type I, collagen type IV, fibronectin, and Snail induced by IL-6 was dramatically decreased in the S3I-201-treated group (Figure 5B–D). Taken together, these data suggested that JAK1/STAT3 signaling is involved in IL-6-induced RPE proliferation and EMT, and blockade of JAK1/STAT3 signaling can reverse the proliferation of RPE cells and EMT.

IL-6 is dramatically upregulated and JAK1/STAT3 signaling is activated in the mouse PVR model in vivo: Based on the results in vitro, we investigated whether the IL-6/JAK1/STAT3 signaling pathway is involved in PVR in vivo using the dispase/collagenase-induced PVR model. First, we examined the expression of IL-6 and gp130 in the retinas of the PVR mice. The results from the quantitative real-time PCR showed IL-6 was rapidly increased by 94-fold at day 1 after dispase/collagenase injection, and then declined gradually and returned to the baseline at day 14 (Figure 6A). Meanwhile, the expression of gp130 was also increased by 2.3-fold at day 1 after injection, reached maximum (−3.5-fold) at day 7, and maintained at 14 days (Figure 6A). The western blotting results also illustrated that IL-6 and gp130 were upregulated markedly at day 1 after PVR induction (Figure 6B,C). Then, we examined whether JAK/STAT3 signaling was activated during PVR in vivo. We found that the phosphorylation of JAK1 and STAT3 was distinctly increased at 24 h in PVR (Figure 6D,E). Therefore, these results implied that the IL-6/JAK1/STAT3 signaling pathway is involved in the pathogenesis of PVR in vivo.

IL-6 deficiency statistically significantly prevents PVR progression in vivo: Finally, we investigated whether IL-6 deficiency could prevent dispase/collagenase-induced PVR in vivo using IL-$6^{-/-}$ mice. As shown in Figure 7A, hematoxylin and eosin staining of cross sections of the eyeballs displayed that the control eyes appeared histologically normal with distinct retinal layers, while the WT mice presented poorly distinguishable retinal layers, numerous inflammatory cell infiltration in the retinal ganglion cell layer and inner

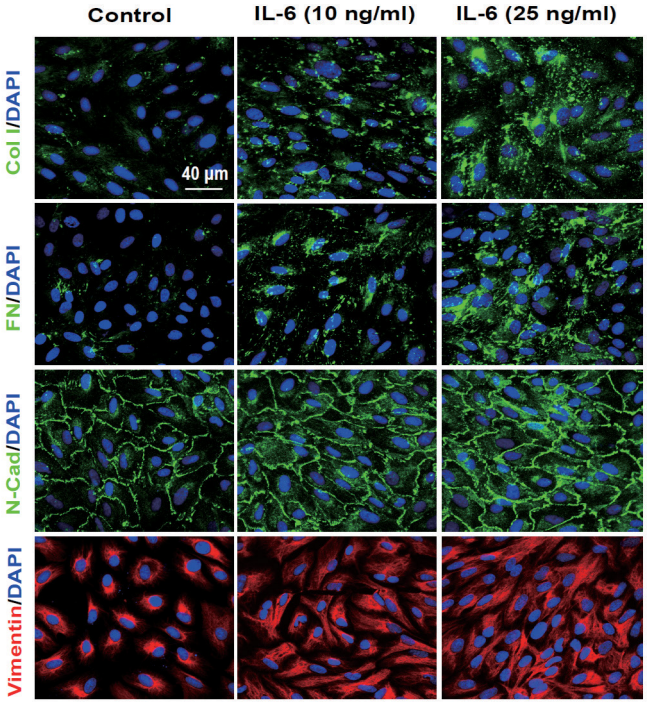

Figure 2. IL-6 induces the expression of EMT markers and cytoskeletal reorganization in RPE cells. The expression of the epithelial-mesenchymal transition (EMT) markers collagen type I, fibronectin, N-cadherin, and vimentin was examined with immunofluorescence staining after RPE cells were exposed to 10 and 25 ng/ml of interleukin-6 (IL-6) for 48 h. Scale bars: 40 μm.

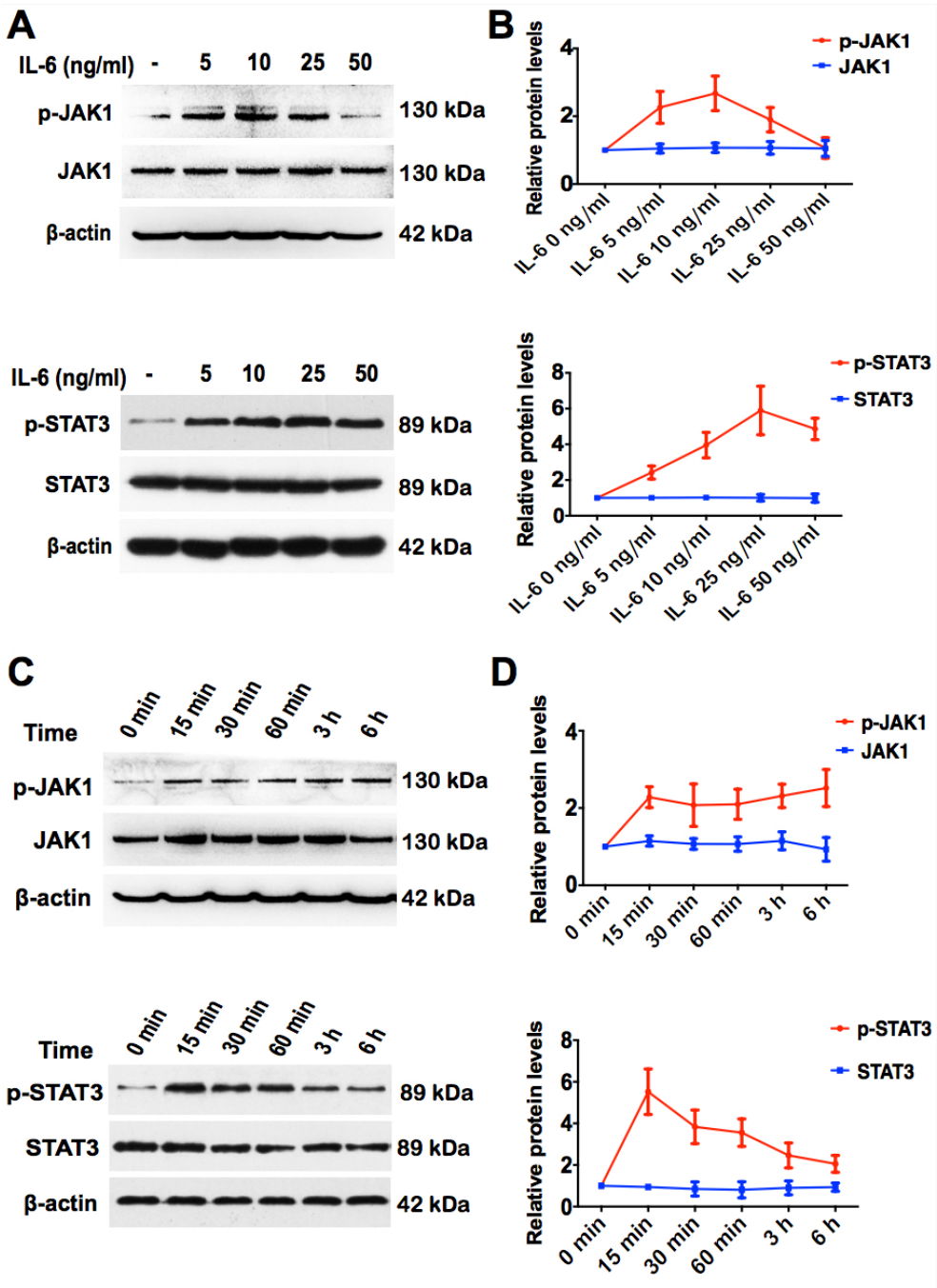

Figure 3. JAK1/STAT3 signaling is activated by IL-6 in RPE cells. RPE cells were cultured with various concentrations of interleukin-6 (IL-6; 5, 10, 25, and 50 ng/ml) for 60 min. **A**: The protein expression of p-JAK1, JAK1, p-STAT3, and STAT3 was determined with western blotting. **B**: Quantification of p-JAK1, JAK1, p-STAT3, and STAT3 protein levels from three independent experiments. RPE cells were cultured with 25 ng/ml of IL-6 for different times, and p-JAK1, JAK1, p-STAT3, and STAT3 expression was determined with western blotting. **C**: Representative results from one of the three independent experiments are presented. **D**: Quantification of p-JAK1, JAK1, p-STAT3, and STAT3 protein levels from three independent experiments.

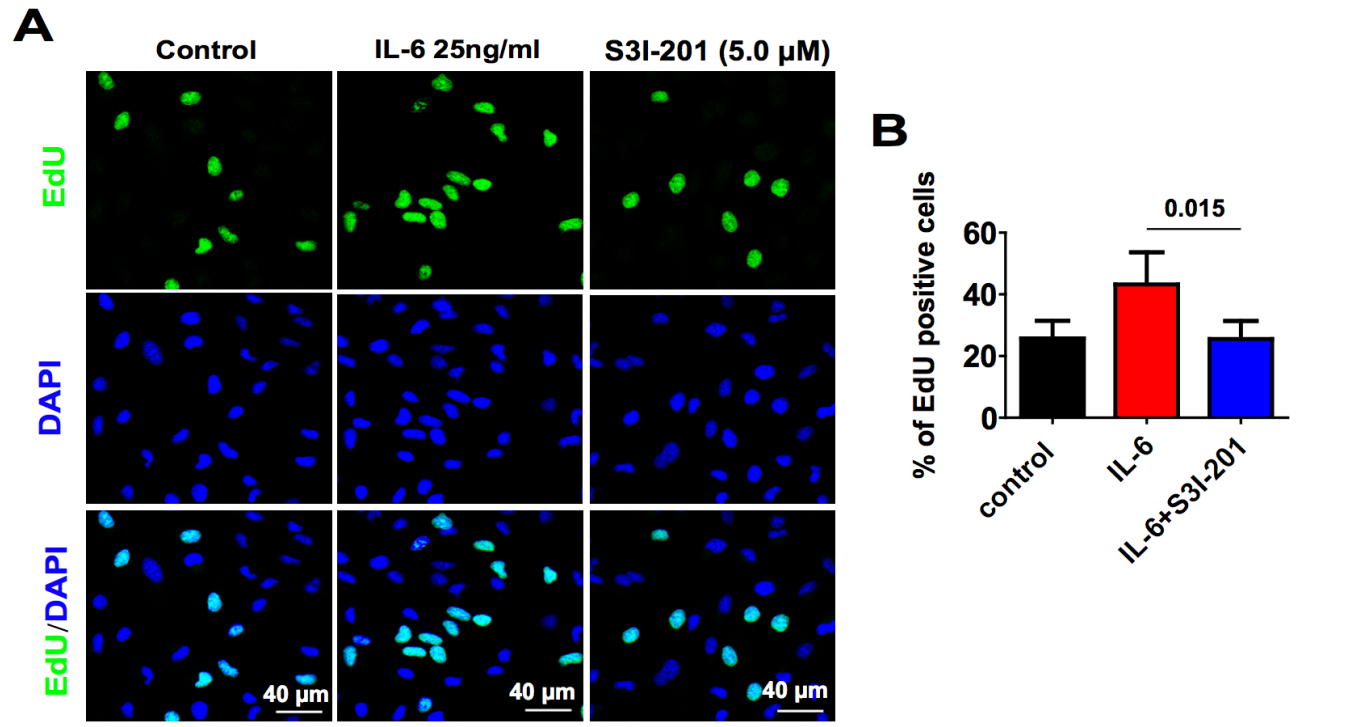

Figure 4. Proliferation of RPE cells is inhibited by blocking IL-6/JAK1/STAT3 signaling. **A**: EdU staining analysis of proliferation of RPE cells after interleukin-6 (IL-6) stimulation with or without S3I-201 (5.0 μM) for 48 h. Scale bars: 40 μm. **B**: Quantification of EdU-positive cells (n = 24 randomized fields per group). P value versus the IL-6 treated group is shown (one-way analysis of variance [ANOVA] with the Tukey-Kramer multiple comparison test).

nuclear layer, extensive retinal folds, retinal detachment, and subretinal fibrosis at 7 days after an intravitreal injection of dispase/collagenase. Nevertheless, the manifestation of PVR was dramatically attenuated in the IL-6$^{-/-}$ mice. No obvious inflammatory cell infiltration in the retina and subretinal fibrosis were observed in the retinas of the IL-6$^{-/-}$ mice. Although localized retinal folds were still presented, the retinal layers were clearly visible in the IL-6$^{-/-}$ mice (Figure 7A). Furthermore, we examined the expression of IL-6, gp130, and EMT markers for 7 days after the PVR model was established. As expected, the results of quantitative real-time PCR and western blotting demonstrated that IL-6, gp130, and EMT markers α-SMA, fibronectin, extracellular matrix (Ecm), collagen type IV, and Snail were distinctly induced in the PVR model in the WT mice, especially α-SMA. Conversely, IL-6 deficiency dramatically decreased their expression at the mRNA and protein levels (Figure 7B–D). Collectively, these data suggest that IL-6 deficiency can effectively prevent development of PVR in vivo.

DISCUSSION

Proliferative vitreoretinopathy, a scarring process that develops with some rhegmatogenous retinal detachments (RRDs), is the most common factor causing surgical failure after treatment [24]. The exact molecular mechanism of PVR pathogenesis remains elusive, but it is associated with the complex interactions between several cell types (e.g., RPE cells, glial cells, and bone marrow–derived cells) and the inflammatory microenvironment. In the present study, we revealed for the first time that IL-6 could markedly promote RPE cell proliferation and EMT through activating the JAK1/STAT3 signaling pathway in vitro. The expression levels of IL-6 and its key receptor subunit gp-130 were dramatically upregulated in the mouse PVR model, which induced activation of the JAK1/STAT3 signaling pathway during pathogenesis. Finally, we validated that IL-6 deficiency and blockade of JAK1/STAT3 signaling could significantly inhibit the proliferation of RPE cells and EMT, and thus, reduce PVR severity. Taken together, these findings support the notion that IL-6 is a key regulator inducing PVR through the JAK1/STAT3 signaling axis.

As a pleiotropic proinflammatory cytokine, IL-6 has been documented to promote fibrosis in several systemic and ocular diseases, including pulmonary fibrosis [25], renal interstitial fibrosis [26], conjunctival fibrosis after glaucoma surgery [27], trachoma related scarring [28], and posterior capsular opacification [29]. After retinal detachment, sustained sterile inflammation and increased levels of cytokines are major factors contributing to the onset of PVR in patients with RRD [30]. Among the increased cytokines, multilevel evidence has proven the possible role of IL-6 in pathogenesis of PVR. For example, the Retina 4 Project and other genetic association studies observed differences in genotype distributions within IL-6 were significantly associated with PVR risk in RD eyes [31-33]. In biomarker analysis,

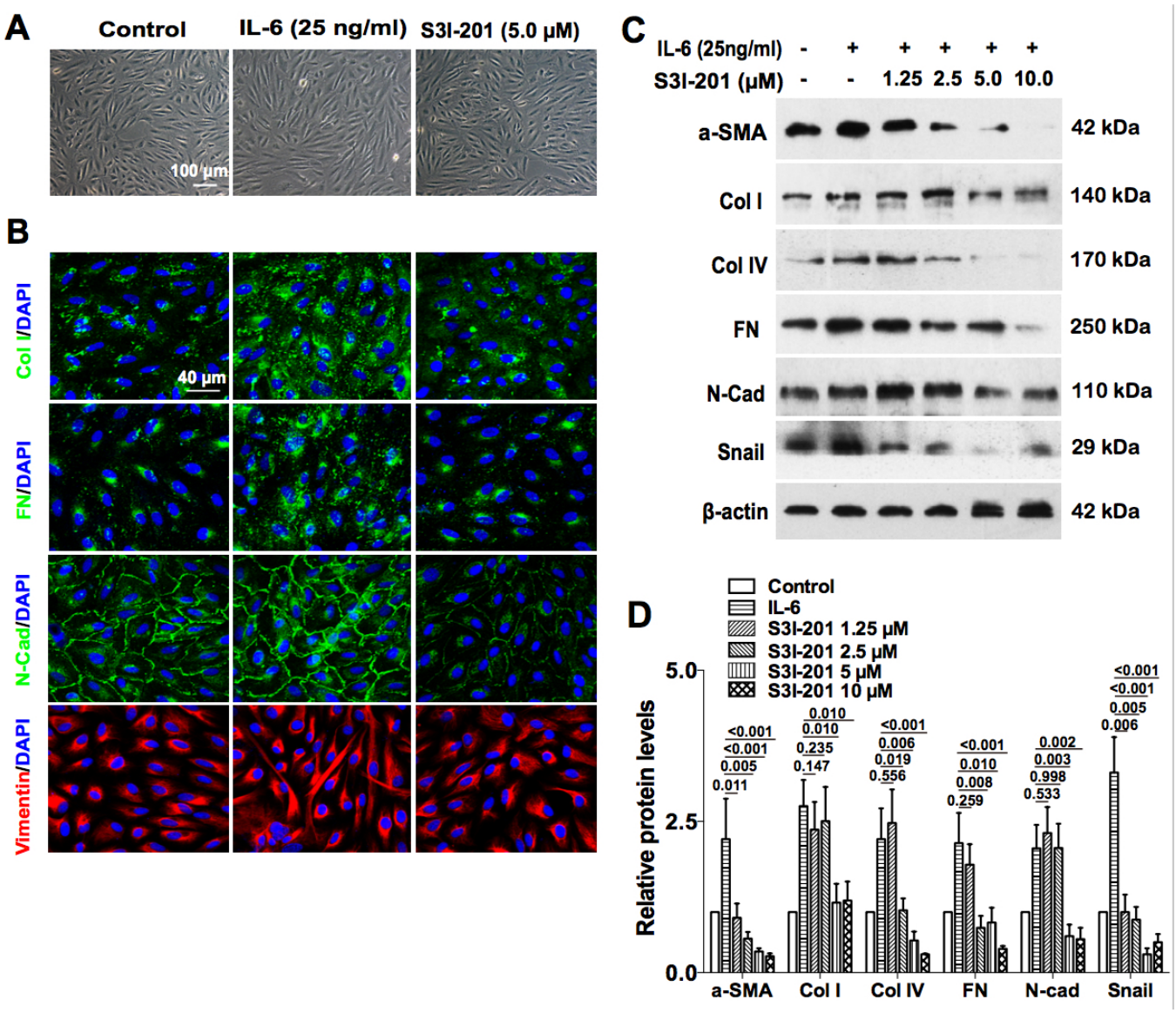

Figure 5. EMT phenotype is reversed by blocking IL-6/JAK1/STAT3 signaling in RPE cells. **A**: Microscopic observations of RPE cells exposed to 25 ng/ml of interleukin-6 (IL-6) with or without S3I-201 (5.0 μM) for 48 h. Scale bar: 100 μm. **B**: Immunofluorescent staining of epithelial-mesenchymal transition (EMT) markers collagen type I, fibronectin, N-cadherin, and vimentin expression in RPE cells exposed to 25 ng/ml of IL-6 with or without S3I-201(5.0 μM) for 48 h. Scale bars: 40 μm. **C**: Western blotting of the expression of EMT markers α-SMA, collagen type I, collagen type IV, fibronectin, N-cadherin, and Snail in RPE cells exposed to 25 ng/ml of IL-6 with increasing concentrations of S3I-201 (1.25, 2.5, 5.0, and 10.0 μM) for 48 h. **D**: Quantification of EMT marker protein levels from three independent experiments. P values versus the IL-6 25 ng/ml treatment group are shown (one-way analysis of variance [ANOVA] with the Tukey-Kramer multiple comparison test).

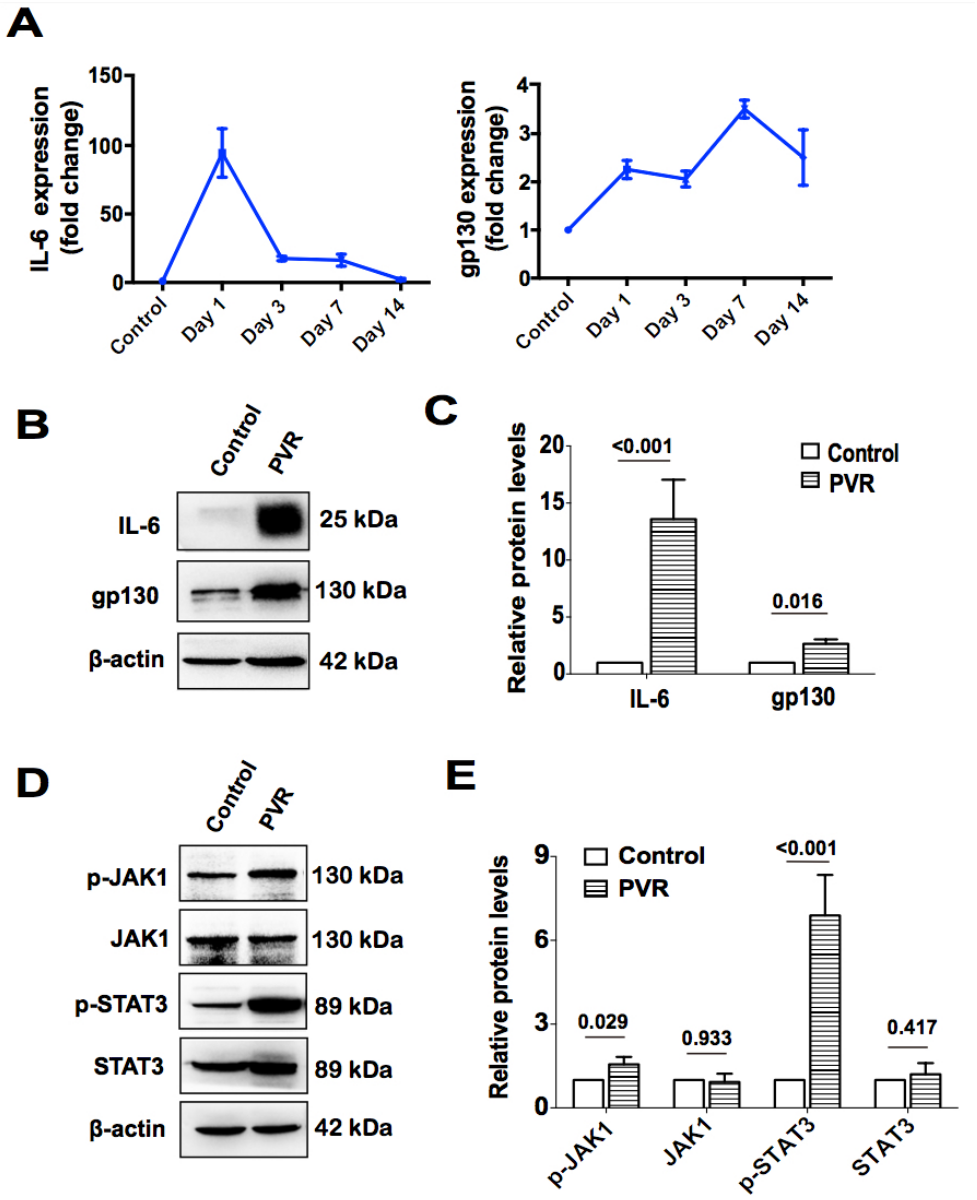

Figure 6. IL-6 is dramatically upregulated and JAK1/STAT3 signaling is activated in the mouse PVR model in vivo. The mouse model of proliferative vitreoretinopathy (PVR) was induced with intravitreal injection of 1 µl of dispase/collagenase at the concentration of 0.02 U/µl in the right eye with a 30 G Hamilton syringe. **A**: Retinas were harvested for quantitative real-time PCR analysis of interleukin-6 (IL-6) and gp130 mRNA levels at day 1, 3, 7, and 14 after injection. **B**: Western blotting of the expression of IL-6 and gp130 protein levels at day 1 after injection. **C**: Quantification of IL-6 and gp130 protein levels from three independent experiments. P values versus the control group are shown (Student *t* test). **D**: Western blotting of the expression of p-JAK1, JAK1, p-STAT3, and STAT3 levels at day 1 after injection. Quantification of the p-JAK1, JAK1, p-STAT3, and STAT3 protein levels from three independent experiments. **E**: P values versus the control group are shown (Student *t* test).

studies have consistently shown that the concentration of IL-6 is elevated in intraocular fluids (i.e., aqueous humor, vitreous, and subretinal fluid) from RRD and PVR eyes compared with healthy controls [20,34,35]. Some of these studies also showed the IL-6 level was positively correlated with the extent of detachment and the risk of PVR incidence [34,36]. In this animal study using a mouse PVR model, we confirmed that mRNA and protein expression of IL-6 and gp130 experienced dramatic changes within 1 day after modeling, indicating that IL-6 and its downstream signaling pathway might participate in the acute-phase response to retinal injuries.

Despite the evidence of high IL-6 levels in PVR eyes, the question remains how IL-6 regulates PVR pathogenesis. A crucial event of fibrotic membrane development is the dedifferentiation of RPE cells into contractile myofibroblasts [2], which involves a basic biologic process, EMT, a common pathophysiological feature underlying several systemic and ocular fibrotic diseases, such as anterior subcapsular cataract [37] and PVR [2,38]. Several growth factor–related signaling pathways (e.g., TGF-β, EGF, and Notch) may induce EMT during embryogenesis, fibrosis, and cancer progression [39]. In this in vitro study, treating RPE cells with IL-6 alone could induce profound morphological changes from the epithelial to the mesenchymal phenotype, accompanied by significant upregulation of mesenchymal markers and transcription factors. It indicated that a high IL-6 level alone might be

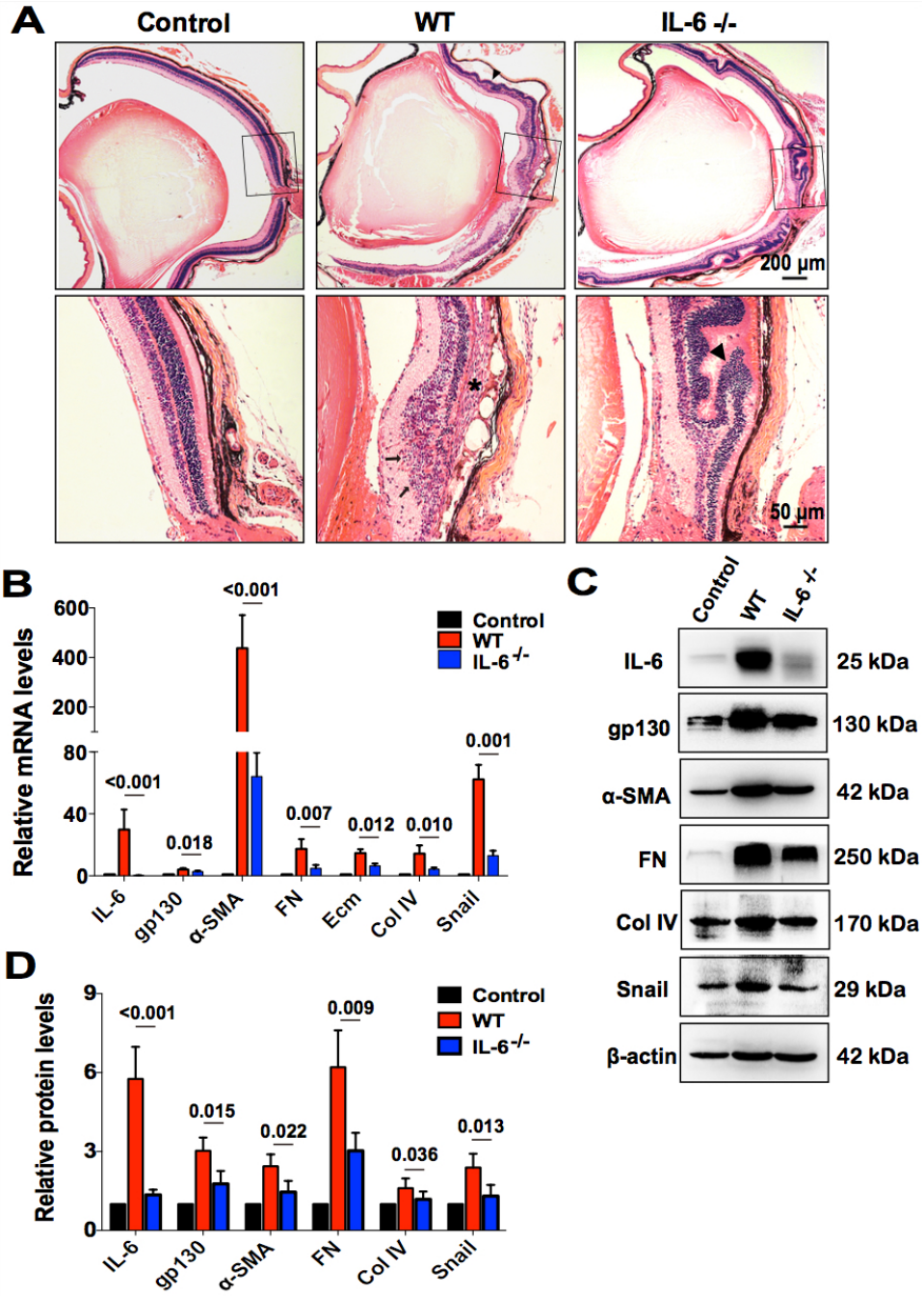

Figure 7. IL-6 deficiency significantly prevents PVR progression in vivo. The proliferative vitreoretinopathy (PVR) model was induced in wild-type (WT) and interleukin-6 (IL-6) −/− mice with intravitreal injection of dispase/collagenase for 7 days. **A**: Representative hematoxylin and eosin staining images of cross sections of the eyeballs display that the WT mice presented poorly distinguishable retinal layers, numerous inflammatory cell infiltration (arrow) in the retinal ganglion cell layer and inner nuclear layer, extensive retinal folds (▲), retinal detachment, and subretinal fibrosis (*). Nevertheless, no obvious inflammatory cell infiltration and subretinal fibrosis were observed in the retinas of the IL-6 −/− mice. Although localized retinal folds are still presented, the retinal layers are clearly visible in the IL-6 −/− mice. Retinas were harvested for quantitative real-time PCR analysis of the expression of IL-6, gp130, and epithelial-mesenchymal transition (EMT) markers. **B**: P values compared with the WT group are shown (one-way analysis of variance [ANOVA] with the Tukey-Kramer multiple comparison test). **C**: Retinas were harvested for western blotting of the expression of IL-6, gp130, and EMT markers. **D**: Quantification of IL-6, gp130, and EMT marker protein levels from three independent experiments. P values versus the WT group are shown (one-way ANOVA with the Tukey-Kramer multiple comparison test).

sufficient to regulate RPE cell dedifferentiating to fibroblasts. This effect of IL-6 on EMT was previously observed in several human cancers, including cervical carcinoma [40], breast cancer cells [41], esophageal adenocarcinoma [42], and colorectal cancer [43], but it was observed in PVR and RPE cells for the first time.

Classical signal transduction of IL-6 involves the activation of JAK family members, and the transcription factors STAT family. IL-6 may also activate the MAPK cascades in the non-canonical pathway. Literature has documented that IL-6 might induce EMT via activating either JAK1 or JAK2 [29,43,44]. In RPE cells, the present in vitro analysis demonstrated that JAK1, rather than JAK2, was phosphorylated immediately upon IL-6 treatment. Combined with the findings that the inhibitor S3I-201 attenuated cell proliferation and morphological changes, we believe that the activation of JAK1/STAT3 mediates the effect of IL-6 on proliferation and EMT in RPE cells.

Agents targeting and modulating the IL-6/JAK/STAT3 pathway have been approved by the U.S. Food and Drug Administration (FDA) for the treatment of several inflammatory conditions and malignancies [45]. Owing to involvement in multiple aspects of fibrosis, IL-6 has emerged as a therapeutic target for many fibrotic diseases as well [46,47]. For example, blockade of IL-6Rα with tocilizumab could profoundly inactivate fibroblast phenotype in skin fibrosis [48]. In a mouse RD model induced by subretinal injection of hyaluronic acid, a previous study demonstrated blocking IL-6 signaling with a monoclonal antibody against gp130 can reduce monocyte infiltrating to the vitreoretinal interface [49]. In the present study, we investigated the antifibrosis effect of blockade of IL-6 using the experimental PVR model induced by intravitreal injection of dispase in the IL-6$^{-/-}$ mice. Compared to the subretinal injection of the hyaluronic acid-induced RD model [50-52], the dispase-induced PVR model has been widely used for its reproducible induction of typical PVR-like lesions, for example, the appearance of extensive retinal folds, the formation of large widespread epi- and subretinal membranes, and tractional retinal detachment in rabbits and mice [53]. Using the PVR model, we validated that IL-6 knockout could markedly reduce the severity of PVR. In conjunction with the in vitro findings of the JAK/STAT3 inhibitor on RPE phenotypes, this study implied that blockade of the IL-6/JAK/STAT3 signaling pathway might be beneficial for alleviating inflammation and reducing the risk of PVR incidence after RRD.

In summary, using cultured cells in vitro and the dispase/collagenase-induced mouse PVR model, the present results provide, for the first time, evidence that IL-6 and the JAK1/STAT3 pathway play important roles in PVR. IL-6 promotes RPE cell proliferation, EMT, and PVR progression in vitro and in vivo via activating the JAK1/STAT3 signaling pathway. However, blockade of the JAK1/STAT3 pathway and IL-6 deficiency can inhibit proliferation of RPE cells, EMT, and PVR progression. The present data suggest that IL-6 deficiency and blockade of the JAK1/STAT3 pathway may be promising strategies in the prevention and treatment of PVR.

APPENDIX 1. STR ANALYSIS.

To access the data, click or select the words "Appendix 1."

ACKNOWLEDGMENTS

The present work was supported by the Natural Science Foundation of Guangdong Province (2016A030310230, 2017A030313802), and the National Natural Science Foundation of China (81600751, 81700820). **Contributors:** Conception and design of the study: Wei Xiao and Xiaoyun Chen. Data collection: Xiaoyun Chen, Weimin Yang and Xiaoqian Deng. Data analysis and interpretation: Xiaoyun Chen, Shaobi Ye and Wei Xiao. Drafting the article: Xiaoyun Chen. Critical revision of the manuscript: Wei Xiao. Final approval of the version to be published: all authors.

REFERENCES

1. Pastor JC. Proliferative vitreoretinopathy: an overview. Surv Ophthalmol 1998; 43:3-18. [PMID: 9716190].

2. Pastor JC, de la Rua ER, Martin F. Proliferative vitreoretinopathy: risk factors and pathobiology. Prog Retin Eye Res 2002; 21:127-44. [PMID: 11906814].

3. Kroll P, Rodrigues EB, Hoerle S. Pathogenesis and classification of proliferative diabetic vitreoretinopathy. Ophthalmologica 2007; 221:78-94. [PMID: 17380062].

4. Sun JK, Arroyo JG. Adjunctive therapies for proliferative vitreoretinopathy. Int Ophthalmol Clin 2004; 44:1-10. [PMID: 15211172].

5. Yang S, Li H, Li M, Wang F. Mechanisms of epithelial-mesenchymal transition in proliferative vitreoretinopathy. Discov Med 2015; 20:207-17. [PMID: 26562474].

6. Machemer R, van Horn D, Aaberg TM. Pigment epithelial proliferation in human retinal detachment with massive periretinal proliferation. Am J Ophthalmol 1978; 85:181-91. [PMID: 623188].

7. Lei H, Rheaume MA, Kazlauskas A. Recent developments in our understanding of how platelet-derived growth factor (PDGF) and its receptors contribute to proliferative vitreoretinopathy. Exp Eye Res 2010; 90:376-81. [PMID: 19931527].

8. Chiba C. The retinal pigment epithelium: an important player of retinal disorders and regeneration. Exp Eye Res 2014; 123:107-14. [PMID: 23880527].

9. Tosi GM, Marigliani D, Romeo N, Toti P. Disease pathways in proliferative vitreoretinopathy: an ongoing challenge. J Cell Physiol 2014; 229:1577-83. [PMID: 24604697].

10. Wang SW, Sun YM. The IL-6/JAK/STAT3 pathway: potential therapeutic strategies in treating colorectal cancer Int J Oncol 2014; 44:1032-40. Review[PMID: 24430672].

11. Schaper F, Rose-John S. Interleukin-6: Biology, signaling and strategies of blockade. Cytokine Growth Factor Rev 2015; 26:475-87. [PMID: 26189695].

12. Rose-John S. IL-6 trans-signaling via the soluble IL-6 receptor: importance for the pro-inflammatory activities of IL-6. Int J Biol Sci 2012; 8:1237-47. [PMID: 23136552].

13. Hunter CA, Jones SA. IL-6 as a keystone cytokine in health and disease. Nat Immunol 2015; 16:448-57. [PMID: 25898198].

14. Jones SA, Scheller J, Rose-John S. Therapeutic strategies for the clinical blockade of IL-6/gp130 signaling. J Clin Invest 2011; 121:3375-83. [PMID: 21881215].

15. Jones SA. Directing transition from innate to acquired immunity: defining a role for IL-6. J Immunol 2005; 175:3463-8. [PMID: 16148087].

16. Noma H, Funatsu H, Mimura T, Harino S, Hori S. Vitreous levels of interleukin-6 and vascular endothelial growth factor in macular edema with central retinal vein occlusion. Ophthalmology 2009; 116:87-93. [PMID: 19118700].

17. Jonas JB, Tao Y, Neumaier M, Findeisen P. Cytokine concentration in aqueous humour of eyes with exudative age-related macular degeneration. Acta Ophthalmol 2012; 90:e381-8. [PMID: 22490043].

18. Ma Y, Tao Y, Lu Q, Jiang YR. Intraocular expression of serum amyloid a and interleukin-6 in proliferative diabetic retinopathy. Am J Ophthalmol 2011; 152:678-85. .

19. Bastiaans J, van Meurs JC, Mulder VC, Nagtzaam NM, Smitste Nijenhuis M, Dufour-van den Goorbergh DC, van Hagen PM, Hooijkaas H, Dik WA. The role of thrombin in proliferative vitreoretinopathy. Invest Ophthalmol Vis Sci 2014; 55:4659-66. [PMID: 25015355].

20. Symeonidis C, Papakonstantinou E, Androudi S, Georgalas I, Rotsos T, Karakiulakis G, Diza E, Dimitrakos SA. Comparison of interleukin-6 and matrix metalloproteinase expression in the subretinal fluid and the vitreous during proliferative vitreoretinopathy: correlations with extent, duration of RRD and PVR grade. Cytokine 2014; 67:71-6. [PMID: 24725542].

21. Chen X, Xiao W, Chen W, Liu X, Wu M, Bo Q, Luo Y, Ye S, Cao Y, Liu Y. MicroRNA-26a and −26b inhibit lens fibrosis and cataract by negatively regulating Jagged-1/Notch signaling pathway. Cell Death Differ 2017; 24:1990-[PMID: 28937685].

22. Canto Soler MV, Gallo JE, Dodds RA, Suburo AM. A mouse model of proliferative vitreoretinopathy induced by dispase. Exp Eye Res 2002; 75:491-504. [PMID: 12457862].

23. Johnson DE, O'Keefe RA, Grandis JR. Targeting the IL-6/JAK/STAT3 signalling axis in cancer. Nat Rev Clin Oncol 2018; 15:234-48. [PMID: 29405201].

24. Pastor JC, de la Rua ER, Martin F. Proliferative vitreoretinopathy: risk factors and pathobiology. Prog Retin Eye Res 2002; 21:127-44. [PMID: 11906814].

25. Papiris SA, Tomos IP, Karakatsani A, Spathis A, Korbila I, Analitis A, Kolilekas L, Kagouridis K, Loukides S, Karakitsos P, Manali ED. High levels of IL-6 and IL-8 characterize early-on idiopathic pulmonary fibrosis acute exacerbations. Cytokine 2018; 102:168-72. [PMID: 28847533].

26. Yang J, Chen J, Yan J, Zhang L, Chen G, He L, Wang Y. Effect of interleukin 6 deficiency on renal interstitial fibrosis. PLoS One 2012; 7:e52415-[PMID: 23272241].

27. Yu-Wai-Man C, Tagalakis AD, Meng J, Bouremel Y, Lee RMH, Virasami A, Hart SL, Khaw PT. Genotype-Phenotype Associations of IL-6 and PRG4 With Conjunctival Fibrosis After Glaucoma Surgery. JAMA Ophthalmol 2017; 135:1147-55. [PMID: 28975281].

28. Kechagia JZ, Ezra DG, Burton MJ, Bailly M. Fibroblasts profiling in scarring trachoma identifies IL-6 as a functional component of a fibroblast-macrophage pro-fibrotic and pro-inflammatory feedback loop. Sci Rep 2016; 6:28261-[PMID: 27321784].

29. Ma B, Yang L, Jing R, Liu J, Quan Y, Hui Q, Li J, Qin L, Pei C. Effects of Interleukin-6 on posterior capsular opacification. Exp Eye Res 2018; 172:94-103. [PMID: 29617629].

30. Pastor JC, Rojas J, Pastor-Idoate S, Di Lauro S, Gonzalez-Buendia L, Delgado-Tirado S. Proliferative vitreoretinopathy: A new concept of disease pathogenesis and practical consequences. Prog Retin Eye Res 2016; 51:125-55. [PMID: 26209346].

31. Lumi X, Jelen MM, Zupan A, Bostjancic E, Ravnik-Glavac M, Hawlina M, Glavac D. Single Nucleotide Polymorphisms in Retinal Detachment Patients with and without Proliferative Vitreoretinopathy. Retina 2019; 5:811-818. [PMID: 30807515].

32. Rojas J, Fernandez I, Pastor JC, Maclaren RE, Ramkissoon Y, Harsum S, Charteris DG, Van Meurs JC, Amarakoon S, Ruiz-Moreno JM, Rocha-Sousa A, Brion M, Carracedo A. A genetic case-control study confirms the implication of SMAD7 and TNF locus in the development of proliferative vitreoretinopathy. Invest Ophthalmol Vis Sci 2013; 54:1665-78. [PMID: 23258148].

33. Rojas J, Fernandez I, Pastor JC, Garcia-Gutierrez MT, Sanabria RM, Brion M, Sobrino B, Manzanas L, Giraldo A, Rodriguez-de la Rua E, Carracedo A. Development of predictive models of proliferative vitreoretinopathy based on genetic variables: the Retina 4 project. Invest Ophthalmol Vis Sci 2009; 50:2384-90. [PMID: 19098314].

34. Kiang L, Ross BX, Yao J, Shanmugam S, Andrews CA, Hansen S, Besirli CG, Zacks DN, Abcouwer SF. Vitreous Cytokine Expression and a Murine Model Suggest a Key Role of Microglia in the Inflammatory Response to Retinal

Detachment. Invest Ophthalmol Vis Sci 2018; 59:3767-78. [PMID: 30046818].

35. Kunikata H, Yasuda M, Aizawa N, Tanaka Y, Abe T, Nakazawa T. Intraocular concentrations of cytokines and chemokines in rhegmatogenous retinal detachment and the effect of intravitreal triamcinolone acetonide. Am J Ophthalmol 2013; 155:1028-37. .

36. Ricker LJ, Kijlstra A, Kessels AG, de Jager W, Liem AT, Hendrikse F, La Heij EC. Interleukin and growth factor levels in subretinal fluid in rhegmatogenous retinal detachment: a case-control study. PLoS One 2011; 6:e19141-[PMID: 21556354].

37. Xiao W, Chen X, Li W, Ye S, Wang W, Luo L, Liu Y. Quantitative analysis of injury-induced anterior subcapsular cataract in the mouse: a model of lens epithelial cells proliferation and epithelial-mesenchymal transition. Sci Rep 2015; 5:8362-[PMID: 25666271].

38. Xiao W, Chen X, Liu X, Luo L, Ye S, Liu Y. Trichostatin A, a histone deacetylase inhibitor, suppresses proliferation and epithelial-mesenchymal transition in retinal pigment epithelium cells. J Cell Mol Med 2014; 18:646-55. [PMID: 24456602].

39. Kalluri R, Weinberg RA. The basics of epithelial-mesenchymal transition. J Clin Invest 2009; 119:1420-8. [PMID: 19487818].

40. Miao JW, Liu LJ, Huang J. Interleukin-6-induced epithelial-mesenchymal transition through signal transducer and activator of transcription 3 in human cervical carcinoma. Int J Oncol 2014; 45:165-76. [PMID: 24806843].

41. Gyamfi J, Lee YH, Eom M, Choi J. Interleukin-6/STAT3 signalling regulates adipocyte induced epithelial-mesenchymal transition in breast cancer cells. Sci Rep 2018; 8:8859-[PMID: 29891854].

42. Ebbing EA, van der Zalm AP, Steins A, Creemers A, Hermsen S, Rentenaar R, Klein M, Waasdorp C, Hooijer GKJ, Meijer SL, Krishnadath KK, Punt CJA, van Berge Henegouwen MI, Gisbertz SS, van Delden OM, Hulshof M, Medema JP, van Laarhoven HWM, Bijlsma MF. Stromal-derived interleukin 6 drives epithelial-to-mesenchymal transition and therapy resistance in esophageal adenocarcinoma. Proc Natl Acad Sci USA 2019; 116:2237-42. [PMID: 30670657].

43. Zhang X, Hu F, Li G, Yang X, Liu L, Zhang R, Zhang B, Feng Y. Human colorectal cancer-derived mesenchymal stem cells promote colorectal cancer progression through IL-6/JAK2/STAT3 signaling. Cell Death Dis 2018; 9:25-[PMID: 29348540].

44. Xiao J, Gong Y, Chen Y, Yu D, Wang X, Zhang X, Dou Y, Liu D, Cheng G, Lu S, Yuan W, Li Y, Zhao Z. IL-6 promotes epithelial-to-mesenchymal transition of human peritoneal mesothelial cells possibly through the JAK2/STAT3 signaling pathway. Am J Physiol Renal Physiol 2017; 313:F310-8. [PMID: 28490530].

45. Johnson DE, O'Keefe RA, Grandis JR. Targeting the IL-6/JAK/STAT3 signalling axis in cancer. Nat Rev Clin Oncol 2018; 15:234-48. [PMID: 29405201].

46. Garbers C, Rose-John S. Dissecting Interleukin-6 Classic- and Trans-Signaling in Inflammation and Cancer. Methods Mol Biol 2018; 1725:127-40. [PMID: 29322414].

47. Desallais L, Avouac J, Frechet M, Elhai M, Ratsimandresey R, Montes M, Mouhsine H, Do H, Zagury JF, Allanore Y. Targeting IL-6 by both passive or active immunization strategies prevents bleomycin-induced skin fibrosis. Arthritis Res Ther 2014; 16:R157-[PMID: 25059342].

48. Denton CP, Ong VH, Xu S, Chen-Harris H, Modrusan Z, Lafyatis R, Khanna D, Jahreis A, Siegel J, Sornasse T. Therapeutic interleukin-6 blockade reverses transforming growth factor-beta pathway activation in dermal fibroblasts: insights from the faSScinate clinical trial in systemic sclerosis. Ann Rheum Dis 2018; 77:1362-71. [PMID: 29853453].

49. Wang X, Miller EB, Goswami M, Zhang P, Ronning KE, Karlen SJ, Zawadzki RJ, Pugh EN Jr, Burns ME. Rapid monocyte infiltration following retinal detachment is dependent on non-canonical IL-6 signaling through gp130. J Neuroinflammation 2017; 14:121-[PMID: 28645275].

50. Mandal N, Lewis GP, Fisher SK, Heegaard S, Prause JU, la Cour M, Vorum H, Honore B. Proteomic Analysis of the Vitreous following Experimental Retinal Detachment in Rabbits. J Ophthalmol 2015; 2015:583040-[PMID: 26664739].

51. Cehofski LJ, Mandal N, Honore B, Vorum H. Analytical platforms in vitreoretinal proteomics. Bioanalysis 2014; 6:3051-66. [PMID: 25496257].

52. Mandal N, Lewis GP, Fisher SK, Heegaard S, Prause JU, la Cour M, Vorum H, Honore B. Protein changes in the retina following experimental retinal detachment in rabbits. Mol Vis 2011; 17:2634-48. [PMID: 22065916].

53. Soler MVC, Gallo JE, Dodds RA, Suburo AM. A mouse model of proliferative vitreoretinopathy induced by dispase. Exp Eye Res 2002; 75:491-504. [PMID: 12457862].

Articles are provided courtesy of Emory University and the Zhongshan Ophthalmic Center, Sun Yat-sen University, P.R. China. The print version of this article was created on 29 July 2020. This reflects all typographical corrections and errata to the article through that date. Details of any changes may be found in the online version of the article.